NMR Study of Rapidly Exchanging Backbone Amide Protons in Staphylococcal Nuclease and the Correlation with Structural and Dynamic Properties

Susumu Mori,*,†,‡ Chitrananda Abeygunawardana,§ Jeremy M. Berg,† and Peter C. M. van Zijl*,†,‡

Contribution from the Johns Hopkins University School of Medicine, Departments of Biophysics and Biophysical Chemistry, Radiology, and Biological Chemistry, 217 Traylor Building, 720 Rutland Avenue, Baltimore, Maryland 21205

Received September 24, 1996. Revised Manuscript Received January 20, 1997[⊗]

Abstract: Exchange rates of rapidly exchanging (>1.0 s^{-1}) backbone amide protons with solvent water in staphylococcal nuclease (SN) were measured at pH 6.03−7.03 with a 2D heteronuclear water exchange filter sequence (WEX II-FHSQC). Comparison of the exchange data with crystal structure data reveals the following: (1) Non-hydrogen-bonding and exposed residues have protection factors (predicted exchange rate in random coil/measured exchange rate) of less than 15 for non-hydrophobic residues and 10 or higher for hydrophobic residues. Among non-hydrophobic residues, Gly tends to have a higher protection factor (10−15), whereas other residues are below 10. (2) Protection factors for buried and non-hydrogen-bonded protons vary over a wide range (6−10^4). Low protection factors (<25) may indicate fluctuations in structure resulting in substantial solvent exposure. (3) Some hydrogen-bonded and buried protons show rapid exchange, and the protection factors are 25−400. This indicates kinetically labile hydrogen bonds and solvent exposure by structural fluctuations. On the other hand, many protons in this category exchange slower than the detection limit (<1.0 s^{-1}) and are mainly observed in α helices and β sheets, or hydrophobic residues. Although a good correlation between NMR exchange measurements and X-ray structural properties was observed, discrepancies were also found for several residues, namely ^{80}Gln, ^{82}Thr, and ^{138}Asn. The measured pH dependence revealed unusual behavior for ^{77}Asn, possibly due to a tightly bound water molecule. Our data indicate that it is possible to use the exchange rates of rapidly exchanging protons as a probe for studying hydrogen bonding, solvent accessibility, or regional kinetic lability of protein structures in solution at physiological pH.

Introduction

Hydrogen bonds of amide protons play an important role in the structure and function of proteins. Usually, the existence of hydrogen bonds is deduced from the spatial geometry obtained from X-ray crystal or NMR solution studies. However, X-ray structures are not always available for proteins of interest, and NMR structures often lack enough resolution to study hydrogen bonds in detail. This is especially true for the N- and C-termini, and for loop and turn regions where NMR structures often do not converge very well. Even if a high-resolution structure is available, it may not be straightforward to extrapolate the data to physiological conditions or to various other conditions of interest. Furthermore, static structure studies do not provide information about the hydrogen bond strengths. This information is particularly important for those amide protons in contact with solvent, where hydrogen bonds are constantly attacked by solvent water and hydroxyl ions and tend to have more dynamic properties.

One of the methods currently available to assess properties of amide protons is the NMR measurement of their exchange rates with solvent protons. If the exchange rates are very close to those of random coils,[1,2] one may conclude that the amide protons are exposed to the solvent and not involved in intramolecular hydrogen bonding. This kind of information is very useful for various types of structural and dynamic studies. For example, if there is a stretch of such rapidly exchanging protons, it can be deduced that the structure of this region is not well-defined.[3] By observing the pH or salt concentration dependence of proton exchange, insight into distribution of electrostatic potentials at the surface of a protein may be obtained.[4−6] Protein−ligand interactions which inevitably occur at protein surface and often involve non-hydrogen-bonded protons are also an intriguing application of these methods.[7−13] Historically, most exchange measurements have been carried out with use of proton−deuterium substitution experiments, which can determine exchange rates well below 0.1−0.01 s^{-1}. Consequently, most exchange studies have concentrated on slowly exchanging protons which provide information on the

† Department of Biophysics and Biophysical Chemistry.
‡ Department of Radiology.
§ Department of Biological Chemistry.
⊗ Abstract published in *Advance ACS Abstracts,* July 1, 1997.

(1) Molday, R. S.; Englander, S. W.; Kallen, R. G. *Biochemistry* **1972**, *11*, 150−158.
(2) Bai, Y.; Milne, J. S.; Mayne, L.; Englander, S. W. *Proteins; Struct., Funct., Genet.* **1993**, *17*, 75−86.
(3) Wagner, G.; Wuthrich, K. *J. Mol. Biol.* **1982**, *160*, 343−361.
(4) Tüchsen, E.; Woodward, C. *J. Mol. Biol.* **1985**, *185*, 421−430.
(5) Delepierre, M.; Dobson, C. M.; Karplus, M.; Poulsen, F. M.; States, D. J.; Wedin, R. E. *J. Mol. Biol.* **1987**, *197*, 111−130.
(6) Christoffersen, M.; Bolvig, S.; Tüchsen, E. *Biochemistry* **1996**, *35*, 2309−2315.
(7) Simon, I.; Tüchsen, E.; Woodward, C. *Biochemistry* **1984**, *23*, 2064−2068.
(8) Seeholzer, S. H.; Wand, A. J. *Biochemistry* **1989**, *28*, 4011−4020.
(9) Paterson, Y.; Englander, S. W.; Roder, H. *Science* **1990**, *249*, 755−759.
(10) Spera, S.; Ikura, M.; Bax, A. *J. Biomol. NMR* **1991**, *1*, 155−165.
(11) Mayne, L.; Paterson, Y.; Cerasoli, D.; Englander, S. W. *Biochemistry* **1992**, *31*, 10678−10685.
(12) Skelton, N. J.; Ködel, J.; Akke, M.; Chazin, W. J. *J. Mol. Biol.* **1992**, *227*, 1100−1117.
(13) Finucane, M. D.; Jardetzky, O. *J. Mol. Biol.* **1995**, *253*, 576−589.

S0002-7863(96)03351-3 CCC: $14.00

exchange mechanisms of buried or highly protected protons and shed light on global and local unfolding events. However, most non-hydrogen-bonded protons as well as weakly hydrogen-bonded protons exchange within the dead time of conventional experiments. In order to circumvent this problem, extreme conditions (e.g. low pH or low temperature) or quenching methods have been employed.[3,14−16] However, finite exchange after quenching may still cause errors for rapidly exchanging protons, especially when lengthy two-dimensional experiments are needed for comprehensive assignment. Alternatively, saturation transfer experiments or relaxation measurements combined with two-dimensional detection have also been successfully used to monitor rapidly exchanging protons.[10,12,13,17] However, these studies require assumption of a uniform T_1 of the amide protons and are prone to inaccuracy due to spin diffusion or intramolecular NOEs from C_α protons at the water frequency. Because of these difficulties, only rough estimates of the exchanging properties of rapidly exchanging protons have been available, especially at physiological conditions. Recently developed 2D water magnetization transfer experiments[18−23] have the ability to measure rapidly exchanging protons (ca. 0.1−100 s^{-1}) precisely and, thus, provide the opportunity to study behavior of exchangeable protons close to or at the surface of proteins.

The purpose of this study is to elucidate the properties of rapidly exchanging amide protons near physiological pH, and to compare the exchange rates with structural and dynamic information obtained by X-ray and NMR studies. For this purpose, we used 1.5 mM staphylococcal nuclease (SN; 149 residues) in the pH range 6.03−7.03. The structure of SN has been solved by X-ray crystallography, and information about solvent accessibility and hydrogen bonds is available.[24] These studies have shown that SN consists of three α helices, five β strands, ten turns, and three loops. These secondary structures have also been confirmed in solution by NMR studies, although greater flexibility in a region around ^{50}Gly is indicated.[25,26] Exchange studies of SN by proton−deuterium substitution have also been published.[25,27] The availability of this structural and dynamic information makes SN a suitable model for further investigation of the properties of rapidly exchanging amide protons. The NMR method used was the WEX II-FHSQC sequence,[23,28] which provides a well-defined mixing time, minimized cancellation errors, negligible radiation damping, and efficient water flip-back that avoids sensitivity losses due to water saturation. The sequence also has the option of spin−echo filtering to estimate contributions of intramolecular NOEs (C_αHs → NHs).[23]

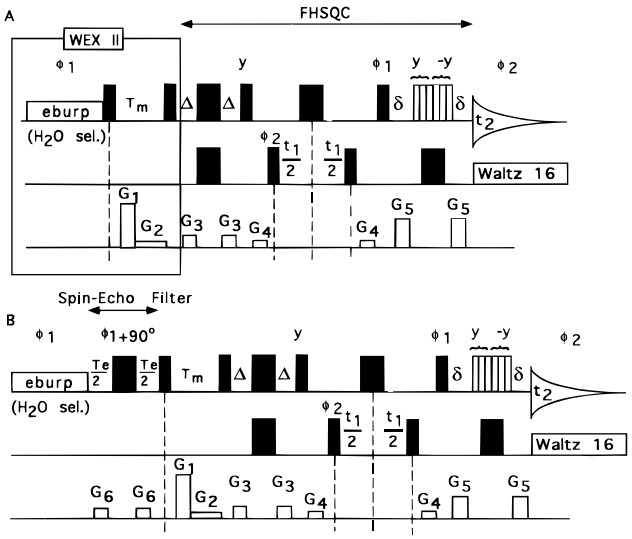

Figure 1. The WEX II-FHSQC sequences. The part of the sequence inside the solid box in part A is the WEX II filter. The first pulse is the 90° water selective pulse (eburp; 16 ms). The composite pulse during *J*-refocussing is a 3−9−19−19−9−3 pulse with intervals of 200 μs. The phases ϕ_1 and ϕ_2 are cycled $\{x, x, -x, -x\}$ and $\{x, -x, x, -x\}$, respectively. T_m is varied from 5 to 50 ms. Contributions of intramolecular NOEs (C_αHs → NHs) can be estimated by the spin−echo filter inserted in the WEX II filter (B). T_e is 40−60 ms. Unless indicated, pulses are applied along the *x* axis. Narrow and wide pulses denote 90° and 180° pulses, respectively. Δ and δ are tuned to get a $^1/_4J_{NH}$ evolution period. Gradients during T_m are 9.0 G/cm × 1 ms (G_1) and 0.1 G/cm for the rest of the T_m period (G_2). G_3 = 2.5 G/cm × 1 ms, G_4 is null, G_5 = 11 G/cm × 1 ms, and G_6 = 1.5 G/cm × 1 ms.

Experimental Section

Figure 1A shows the WEX II-FHSQC NMR pulse sequence. The part of the sequence surrounded by the solid box is the WEX II filter,[22] while the part of the sequence starting with the hard 90° pulse after mixing (T_m) is the FHSQC method.[28] By employing the phase table in the figure legend, water magnetization is flipped back to the *z* axis before the acquisition, thus avoiding signal loss by water saturation. All protein magnetization is excited by the first hard pulse and dephased by the subsequent gradient pulse (G_1). As a result, the magnetization originating from water is the major source of signal at acquisition, and cancellation errors are minimized. Unlike conventional inversion transfer experiments, a clear definition of T_m is obtained (from the first hard pulse to the second hard pulse) and, therefore, initial slope analysis is accurate. As a consequence, the T_1 values of amide protons are not required for rate estimation and the effects of spin diffusion are minimized. Radiation damping is avoided by using dephasing/rephasing gradients when water magnetization is in the transverse plane.

The theory for estimating exchange rates from the signal as a function of T_m has been discussed in detail elsewhere.[20,29,30] Briefly, assuming the molar fraction of H_2O (X_B) to be much higher than that of the protein (X_A), so that $X_B \approx 1$, and neglecting the effect of dipolar coupling (NOE), the T_m dependency of the signal intensity of WEX II-FHSQC peaks (*S*) is given by:

$$S = \frac{fX_A k}{(R_{1A} + k - R_{1B})}(\exp^{(-R_{1B}T_m)} - \exp^{[-(R_{1A}+k)T_m]}) \qquad (1)$$

in which R_1 is the inverse of T_1, *k* is the normalized rate constant (k =

(14) Tüchsen, E.; Woodward, C. *J. Mol. Biol.* **1985**, *185*, 405−419.
(15) Orban, J.; Alexander, P.; Bryan, P.; Khare, D. *Biochemistry* **1995**, *34*, 15291−15300.
(16) Zhang, Y.-Z.; Paterson, Y.; Roder, H. *Protein Sci.* **1995**, *4*, 804−814.
(17) Gryk, M. R.; Finucane, M. D.; Zheng, Z.; Jardetzky, O. *J. Mol. Biol.* **1995**, *246*, 618−627.
(18) Grzesiek, S.; Bax, A. *J. Biomol. NMR* **1993**, *3*, 627−638.
(19) Gemmecker, G.; Hahnke, W.; Kessler, H. *J. Am. Chem. Soc.* **1993**, *115*, 11620−11621.
(20) Mori, S.; Johnson, M. O.; Berg, J. M.; van Zijl, P. C. M. *J. Am. Chem. Soc.* **1994**, *116*, 11982−11984.
(21) Koide, S.; Jahnke, W.; Wright, P. E. *J. Biomol. NMR* **1995**, *6*, 306−312.
(22) Mori, S.; Abeygunawardana, C.; van Zijl, P. C. M.; Berg, J. *J. Magn. Reson. B* **1996**, *110*, 96−101.
(23) Mori, S.; Berg, J. M.; van Zijl, P. C. M. *J. Biomol. NMR* **1996**, *7*, 77−82.
(24) Hynes, T. R.; Fox, R. O. *Proteins; Struct., Funct., Genet.* **1991**, *10*, 92−105.
(25) Torchia, D. A.; Sparks, S. W.; Bax, A. *Biochemistry* **1989**, *28*, 5509−5524.
(26) Kay, L. E.; Torchia, D. A.; Bax, A. *Biochemistry* **1989**, *28*, 8972−8979.
(27) Loh, S. N.; Prehoda, K. E.; Wang, J.; Markley, J. L. *Biochemistry* **1993**, *32*, 11022−11028.
(28) Mori, S.; Abeygunawardana, C.; Johnson, M. O.; Berg, J.; Van Zijl, P. C. M. *J. Magn. Reson. B* **1995**, *108*, 94−98.
(29) Schwartz, A. L.; Cutnell, J. D. *J. Magn. Reson.* **1983**, *53*, 398−411.
(30) Jeener, J.; Meier, B. H.; Bachmann, P.; Ernst, R. R. *J. Chem. Phys.* **1979**, *71*, 4564−4553.

$k_A X_B = k_B X_A$, where k_A and k_B are forward and backward exchange rates from amide protons to water), and f is the proportionality factor between the molar fraction and the signal intensity. The quantity fX_A can be determined from the FHSQC signal intensity (S_{ref}) so that it is factored out by normalizing S by S_{ref}. The quantity R_{1B} (inverse of water T_1) was separately determined to be 0.26 s^{-1} in our protein solution and taken to be pH independent. When determining the T_1 values, we used a 10-s predelay and avoided radiation damping during the inversion delay using a pulsed field gradient. In order to minimize the contribution of spin diffusion, initial slope analysis ($T_m = 5-50$ ms) was used. k and $R_{1A} + k$ can be estimated by two-parameter fitting of the initial slope of the S/S_{ref} curve. In order to perform a WEX II-FHSQC experiment, it is of central importance to confirm minimum water saturation for two reasons. First, all signals observed in the WEX experiment originate from water, and partial saturation of water magnetization directly leads to signal losses. Second, because signal intensities in WEX II-FHSQC experiments (S) have to be normalized by the FHSQC intensities (S_{ref}) for quantitation, the water saturation levels of both experiments must be the same. This can be most easily accomplished by choosing conditions where water saturation is negligible. In this paper, a repetition time (interscan delay + acquisition time) of 2.13 s was used where less than 6% of water is saturated for both WEX II-FHSQC and FHSQC.

Magnetization transfer experiments are prone to artifacts from various sources of NOE effects. The most noticeable artifacts are intramolecular NOEs from protein protons (mostly $C_\alpha H$) excited by the first water-selective excitation pulse to amide protons. The contributions of these intramolecular NOEs can be estimated by using the spin−echo filter, which is inserted between the water-selective pulse and the first hard 90° pulse (Figure 1B).[23] During the spin−echo filter (echo time (T_e): 40−60 ms), water magnetization decreases (denoted by the saturation factor (f_s)) compared with its initial intensity at $T_e = 0$ ms, partly because of T_2 relaxation and partly because of the less efficient water flip-back due to this relaxation. On the other hand, most of the protein magnetization decays away completely because of much shorter T_2 times and J-coupling evolution.[23] Therefore, a signal due entirely to exchange should show signal reduction by a well-defined factor, f_s, for a certain T_e value after the spin−echo filter. When the reduction is more than the factor f_s, NOE contributions are included in the apparent exchange rates (NOE + k). Assuming linear evolution of exchange and NOE signals (initial rate approximation) and complete removal of the NOE effect after the spin−echo filter, the pure exchange rate (k) can be obtained from[23]

$$\frac{k}{\mathrm{NOE} + k} = \frac{S_{s,e}/S}{1 - f_s} \tag{2}$$

where $S_{s,e}$ and S are signal intensities with and without spin−echo filter, respectively. Because NOE + k, $S_{s,e}$, S, and f_s are known values, the pure exchange rate, k, and the NOE contribution can be determined. In this paper, pure exchange rates were determined at two different T_e values (40 and 60 ms) to confirm that the values are independent of T_e and that the assumptions in eq 2 are valid. The saturation factor f_s can be obtained by observing the spin−echo-induced signal loss of amide protons which exchange rapidly enough for k to be dominant compared to the NOE contribution.[23] Alternatively and more easily, f_s can also be reasonably estimated by observing signal loss in Gln and Asn side chain amide protons, because these amide protons are usually well isolated from C_α protons. In our experiments, $f_s = 26\%$ and $f_s = 38\%$ were found for $T_e = 40$ and 60 ms, respectively.

Signals obtained by spin−echo filtering may still contain contributions from intermolecular NOE (water → amide protons). Another source of inaccuracy may arise due to spin diffusion or exchange from rapidly exchanging hydroxyl groups in proteins. Although these contributions are expected to be small compared with those due to the exchange process, they may contaminate the exchange rate measurements, as will be discussed later.

All experiments were carried out with use of a 500 MHz Varian spectrometer equipped with a triple-resonance probe and a single-axis shielded gradient coil. All exchange measurements were carried out with a 1.5 mM ^{15}N-labeled staphylococcal nuclease with no added salt and buffer. Temperature was set to 37 °C. Post-experiment temperature calibration revealed that the actual temperature was 2.4 °C higher than the instrument value.

Results

Amide proton exchange rates of wild-type staphylococcal nuclease (1.5 mM) were measured at pH 6.03, 6.69, and 7.03. The peaks in the $^1H-^{15}N$ HSQC spectrum were assigned according to previously reported chemical shifts[31] and were confirmed by a $^1H-^{15}N$ NOESY-HSQC experiment; 116 of the 149 residues were assigned. Most of the unassigned peaks were clustered at the N-terminus (1−8), C-terminus (144−149), and a flexible loop region (residues 41 to 61). These residues could not be assigned mainly due to chemical shift degeneracy (7.8−8.5 ppm in the proton and 122−126 ppm in the ^{15}N dimension) and/or line broadening due to solvent−protein or conformational exchange. Figure 2A shows a portion of the FHSQC spectrum at pH 7.03 and Figure 2B shows the same region for a WEX II-FHSQC sequence with $T_m = 40$ ms at 5 times magnification. Peaks observed in Figure 2A but not in Figure 2B are due to protons exchanging slower than the detection limit. The peak indicated by an asterisk is from the NH of the Trp side chain. The T_m dependencies of the cross-peak intensities were measured by volume integration except for overlapping peaks which were measured by frequency domain line fitting at the slice of the peak maximum. The exchange rates were estimated by fitting the evolution curve to eq 1. Exchange rates can be reasonably estimated in the range from 1.0 s^{-1} to less than 100 s^{-1} for a 1.5 mM protein sample. The slowest measurable exchange rate is determined by the signal-to-noise ratio and, thus, depends on sample concentration. Finite contribution from spin diffusion also causes inaccuracies when measuring slow exchange. On the other hand, the fastest exchange rate is generally determined by sensitivity and resolution factors in HSQC spectra due to chemical shift degeneracy and/or line broadening. Amide protons exchanging slower than 1.0 s^{-1} were therefore classified as slowly exchanging and not used for quantitative analysis. The average correlation factor for the fitting was 0.996 ± 0.005.

Figure 2C shows the result of the spin−echo filtered WEX II-FHSQC experiment ($T_e = 40$ ms, $T_m = 40$ ms). In this experiment, a longer interscan delay (3.15 s) was used in order to compensate for the reduced efficiency of water flip-back. Notice that the change in the interscan delay reduces f_s, but does not affect the validity of eq 2. By comparing spectra B and C in Figure 2, it can be seen that many peaks observed in spectrum B have significant NOE contributions. For example, amide protons of residues 10, 24, 27, 32, 72, 75, 91, and 95 are totally missing in Figure 2C and are assigned as NOE peaks. The contributions of NOEs on the residues shown in Figure 2C were calculated by using eq 2. If the NOE effect is completely removed by the spin−echo filter, the corrected exchange rates with $T_e = 40$ and 60 ms should be the same. In Figure 3, proton exchange rates obtained at $T_e = 40$ ms are plotted against those at $T_e = 60$ ms. Almost complete agreement between the two measurements can be seen except for a few points near the detection limit (1 s^{-1}). Because the negligible NOE effect at $T_e = 40$ ms is confirmed also at lower pH, only this echo time was used for the experiment at pH 7.03, where the exchange is faster. The average NOE contributions over three different pHs are between 0 and 3.8 s^{-1} (fifth column of Table 1). As expected, these intramolecular NOEs were found to be insensitive to pH changes, as reflected by the small standard deviations. The α-protons that have a chemical shift

(31) Wang, J.; Hinck, A. P.; Loh, S. N.; LeMaster, D. M.; Markley, J. L. *Biochemistry* **1992**, *31*, 921−936.

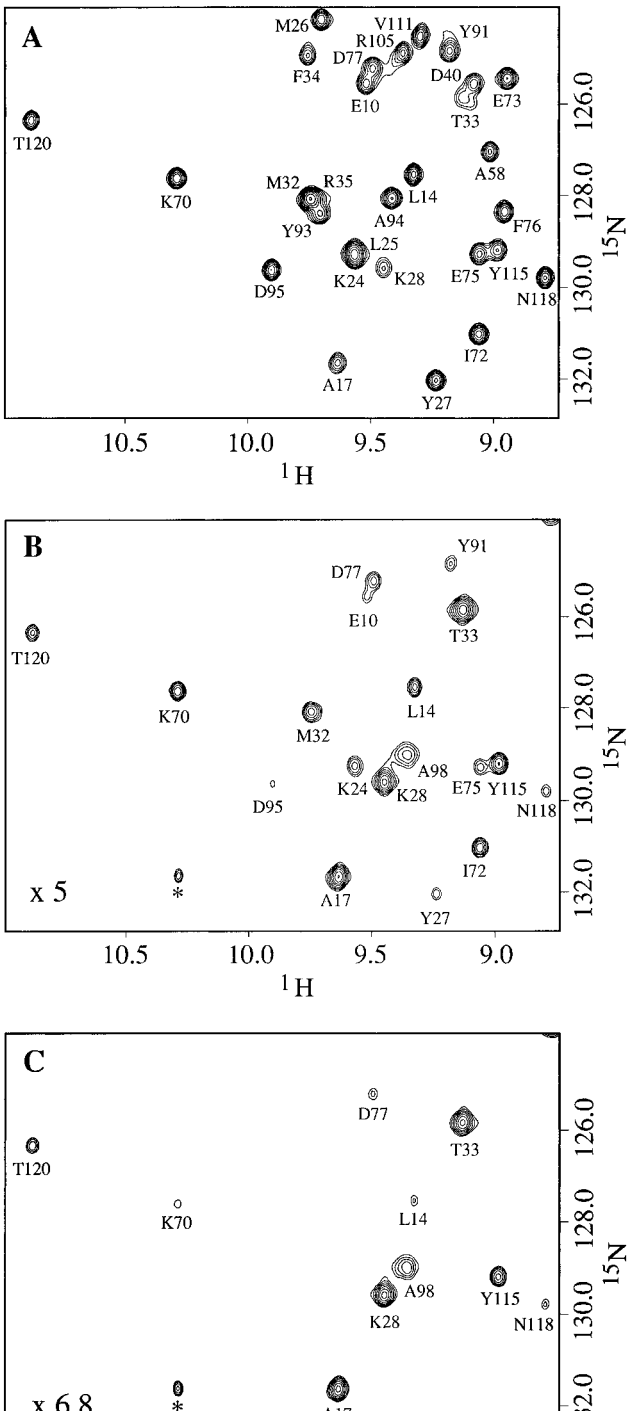

Figure 2. Spectra of 1.5 mM Staphylococcal nuclease (pH 7.03 at 39.4 °C) recorded by the FHSQC (A), WEX II-FHSQC (B), and spin−echo filtered WEX II-FHSQC (C) methods. Only a portion of the 2D spectra is shown. The contour level in part C is at 74% of that in part B in order to compensate for the signal loss by water saturation (f_s) due to the spin−echo filter. T_m = 40 ms and T_e = 40 ms were used. The number of scans is 32. Spectral widths were 7500 and 2000 Hz in t_2 and t_1, respectively. The number of increments in t_1 was 256. The acquisition time was 128 ms. The asterisk denotes the NH of a Trp side chain.

within ±0.2 ppm of the water frequency are indicated by a dagger in column 5 of Table 1. It can be seen that the origin of the NOE contribution can generally be elucidated from the presence of a neighboring C_α proton close to the water resonance. The exchange rates after correction are also shown in Table 1, and showed strong pH dependence. Because of missing assignments, no results for residues 1−8, 41−61, and 144−149 are given.

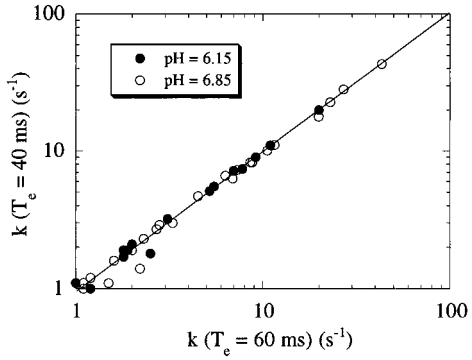

Figure 3. Correlation of pure exchange rates corrected by eq 2 with T_e = 40 (*x*-axis) and 60 ms (*y*-axis).

Discussion

(1) pH Dependence. At a pH of 6 or higher, where amide proton exchange is dominantly catalyzed by hydroxyl ions, exchange rates are expected to be proportional to the concentration of hydroxyl ions. Therefore, from pH 6.03 to 6.69 or from 6.69 to 7.03, exchange rates should increase by factors of 4.6 (=$10^{0.66}$) and 2.2 (=$10^{0.34}$), respectively (total 10 from pH 6.03 to 7.03). The observed average rate increases are 3.3 ± 1.5 from pH 6.03 to 6.69 and 2.0 ± 0.6 from pH 6.69 to 7.03 (total 6.6 from pH 6.03 to 7.03). Thus, a poor pH dependence from pH 6.03 to 6.69 is observed. There are several residues with particularly low pH sensitivity. This can be easily seen from ratios between actual rate increases from pH 6.03 to 7.03 and expected increases, $10^{\Delta pH}$ (=10) shown in the last column of Table 1. The most notable example is residue ^{77}Asn, which shows no pH dependence. Among other residues with weak pH dependence are ^{33}Thr and ^{120}Thr, where the rates increase from pH 6.03 to pH 7.03 by factors of 4 and 2.5, respectively. Residues ^{98}Met, ^{113}Tyr, ^{115}Tyr, and ^{123}Glu also have relatively low pH sensitivity. On the other hand, ^{28}Lys, ^{29}Gly, ^{80}Gln, and ^{81}Arg have rate increases close to the expected values. There are several possible factors which lead to low pH sensitivity. One source of pH-insensitive contributions may arise from NOEs or exchange from intramolecular protein hydroxyl groups. Neither the spin−echo filter nor initial slope analysis can effectively remove this magnetization transfer pathway, because the hydroxyl groups possess water-like NMR properties due to the extremely rapid exchange with water protons (>1000 s^{-1}). Since the amide protons of ^{33}Thr and ^{120}Thr are within 3 Å from their own hydroxyl groups, it is likely that measured exchange rates contain these indirect contributions in addition to exchange from solvent hydroxyl ions.[18] On the other hand, other amide protons with low pH sensitivity do not have any intramolecular hydroxyl group within 6 Å. An alternative explanation is the proximal existence of titratable groups with pK_a of around 6−7, most likely His (pK_a = ca. 6), and possibly Glu and Asp (pK_a = ca. 4). The titration of these groups induces nearby electrostatic potential changes (becomes more negative) as pH increases and affects the catalytic ability of hydroxyl ions.[4−6] In this respect, it may be worthwhile pointing out that, in the crystal structure, residues ^{98}Met, ^{120}Thr, and ^{123}Gln are packed together with ^{121}His and ^{124}His at the surface of the protein, and that a carboxyl group of ^{40}Asp is about 4 Å from the amide proton of ^{113}Tyr. Low pH sensitivity has also been

Table 1. Residue Type, Secondary Structure, NOE Effect, and Exchange Rates of Amide Protons in Staphylococcal Nuclease

					pH 6.03			pH 6.69		pH 7.03		
no.	type	Sec.St.[a]	exposed area[b]	NOE[d]	calcd	k_{obs}[e]	PF[f]	k_{obs}[e]	PF	k_{obs}[e]	PF	ratio[g]
9	K		6.5[c]		16.0	5.5	2.9	NA		NA		
10	E	β		1.6 ± 0.4	2.9	NA						
11	P	β										
12	A	β			3.8	NA		NA		NA		
13	T	β		†	5.7		$>10^3$		$>10^3$		$>10^3$	
14	L	β	4.4[c]	2.7 ± 0.5	2.8			1.2**	10.7	1.9	14.7	
15	I	β			0.8		$>10^3$		$>10^3$		$>10^3$	
16	K	β			3.5		$>10^3$		$>10^3$		$>10^3$	
17	A	β	2.4[c]	2.8 ± 0.5	8.7	1.8	4.8	6.6	6.0	13.3	6.5	0.74
18	I	β			1.2	NA		NA				
19	D	β, turn			2.1	NA		NA				
20	G	turn	*c*		8.3			2.6**	14.7	4.2*	19.8	
21	D	turn	*c*		5.2			1.4**	17.1	3.0*	17.3	
22	T	turn, β			3.9		$>10^4$		$>10^4$		$>10^4$	
23	V	β		†	2.1		$>10^3$		$>10^3$		$>10^3$	
24	K	β		1.9 ± 0.3	4.4		$>10^4$		$>10^4$		$>10^4$	
25	L	β			2.3		$>10^4$		$>10^4$		$>10^4$	
26	M	β		†	4.0		$>10^4$		$>10^4$		$>10^4$	
27	Y	β, turn		2.9 ± 0.4	4.6		$>10^3$		$>10^3$		$>10^3$	
28	K	turn	6.2[c]		6.8	1.7	4.0	8.3	3.7	18.3	3.7	1.08
29	G	turn	4.8[c]		16.0	1.0*	16.0	5.9	12.4	12.5	12.8	1.25
30	Q	turn, β			11.0		$>10^4$		$>10^4$		$>10^4$	
31	P	β		†								
32	M	β		2.4 ± 0.5†	3.7							
33	T	β	4.4[c]	2.9 ± 0.2†	7.3	5.5	1.3	10.3	3.2	22.1	3.3	0.40
34	F	β			6.1		$>10^4$		$>10^4$		$>10^4$	
35	R	β			9.1							
36	L	β			2.9							
37	L			1.2 ± 0.3	1.1		$>10^4$		$>10^4$		$>10^4$	
38	L		6.1[c]		1.1							
39	V		*c*		0.8		$>10^3$		$>10^3$		$>10^3$	
40	D				2.8							
62	T	α			6.6		$>10^4$		$>10^4$		$>10^4$	
63	K	α			9.5	NA		NA		NA		
64	K	α			7.9		$>10^4$		$>10^4$		$>10^4$	
65	M	α			8.5		$>10^4$		$>10^4$		$>10^4$	
66	V	α			1.7		$>10^3$		$>10^3$		$>10^3$	
67	E	α			1.6		$>10^4$		$>10^4$		$>10^4$	
68	N	α		†	15.0							
69	A		*c*	†	14.0							
70	K			3.7 ± 0.2	6.0			1.0**	27.4	1.8*	33.3	
71	K	β		1.3 ± 0.3†	7.9							
72	I	β	4.3[c]	3.8 ± 0.3	1.6					1.3**	12.3	
73	E	β			1.3		$>10^4$		$>10^4$		$>10^4$	
74	V	β		†	1.0		$>10^3$		$>10^3$		$>10^3$	
75	E	β		2.1 ± 0.1	1.6		$>10^4$		$>10^4$		$>10^4$	
76	F	β	1.5[c]	†	2.8							
77	D		0.8[c]	1.6 ± 0.3	4.4	1.8	2.4	1.7	11.8	1.7	25.9	0.1
78	K				4.3							
79	G				16.0					1.4	114.0	
80	Q		*c*		11.0	2.0	5.5	10.5	4.8	17.8	6.2	0.89
81	R		8.7[c]		12.0	4.9	2.5	19.0	2.9	42.2	2.8	0.86
82	T		0.7[c]		9.4			1.0*	43.0	1.9	49.5	
83	D	turn		†	5.5	NA		NA		NA		
84	K	turn	1.8[c]		4.1	NA		NA		NA		
85	Y	turn		†	4.7	NA		NA		NA		
86	G	turn			14.0			1.3	49.2	1.8	77.8	
87	R				12.0					3.7	32.4	
88	G	β		2.5 ± 0.5	20.0							
89	L	β			2.6		$>10^4$		$>10^4$		$>10^4$	
90	A	β		†	4.1		$>10^4$		$>10^4$		$>10^4$	
91	Y	β		2.6 ± 0.3†	3.5		$>10^4$		$>10^4$		$>10^4$	
92	I	β		1.9	1.4		$>10^3$		$>10^3$		$>10^3$	
93	Y	β			2.1		$>10^4$		$>10^4$		$>10^4$	
94	A	β, turn			7.4		$>10^4$		$>10^4$		$>10^4$	
95	D	β, turn		1.5 ± 0.6	3.5							
96	G	turn	3.5[c]		8.3			3.8	10.0	6.0	13.8	
97	K	turn		†	8.9							
98	M	α	9.3[c]	3.2 ± 0.5	8.5	9.3	0.9	30.0	1.3	52.3	1.6	0.56
99	V	α			1.7		$>10^3$		$>10^3$		$>10^3$	
100	N	α	*c*		15.0		$>10^4$		$>10^4$		$>10^4$	
101	E	α	*c*		4.6		$>10^4$		$>10^4$		$>10^4$	
102	A	α			4.9							
103	L	α			1.8							
104	V	α			0.8		$>10^4$		$>10^4$		$>10^4$	
105	R	α			5.7		$>10^3$		$>10^3$		$>10^3$	

Table 1 (Continued)

					pH 6.03			pH 6.69		pH 7.03		
no.	type	Sec.St.[a]	exposed area[b]	NOE[d]	calcd	k_{obs}[e]	PF[f]	k_{obs}[e]	PF	k_{obs}[e]	PF	ratio[g]
106	Q	α			13.0		$>10^4$		$>10^4$		$>10^4$	
107	G				19.0		$>10^3$		$>10^3$		$>10^3$	
108	L				2.6		$>10^3$		$>10^3$		$>10^3$	
109	A		*c*		4.1		$>10^3$		$>10^3$		$>10^3$	
110	K				1.7							
111	V			†	0.9		$>10^3$		$>10^3$		$>10^3$	
112	A			2.9 ± 0.7	4.8							
113	Y		3.6[c]		3.5	3.1*	1.1	8.8	1.8	17.3	2.0	0.56
114	V		4.9[c]		1.5							
115	Y	turn	1.9[c]	1.2 ± 0.2†	2.6	1.0**	2.6	2.7*	4.4	5.5	4.7	0.55
116	K	turn	4.7[c]		6.8	20.0	0.3	F		F		
117	P	turn										
118	N	turn			81.9			1.0**	376.8	2.1	390.0	
119	N	turn			43.0			2.0*	238.0	3.1**	139.0	
120	T	turn			12.0	1.9*	6.3	3.0	18.3	4.8	25.0	0.25
121	H	turn, α			23.0							
122	E	turn, α			5.9							
123	Q	α	0.9[c]		5.6	11.2	0.5	33.2	0.8	70.4	0.8	0.63
124	H	α	1.6[c]		23.0	NA		NA		NA		
125	L	α			4.7		$>10^3$		$>10^3$		$>10^3$	
126	R	α			4.9		$>10^3$		$>10^3$		$>10^3$	
127	K	α			10.0							
128	S	α			20.0							
129	E	α			4.4		$>10^3$		$>10^3$		$>10^3$	
130	A	α			4.9		$>10^3$		$>10^3$		$>10^3$	
131	Q	α			7.6		$>10^3$		$>10^3$		$>10^3$	
132	A	α			10.0		$>10^3$		$>10^3$		$>10^3$	
133	K	α			6.0		$>10^3$		$>10^3$		$>10^3$	
134	K	α			7.9							
135	E	α			2.9		$>10^3$		$>10^3$		$>10^3$	
136	K				4.4		$>10^3$		$>10^3$		$>10^3$	
137	L	turn			2.3		$>10^3$		$>10^3$		$>10^3$	
138	N	turn, turn	1.7[c]		13.0							
139	I	turn, turn			2.6	NA		NA		NA		
140	W	turn, turn			1.5	NA		NA		NA		
141	S	turn			12.0			1.6	34.3	3.3	36.4	
142	E	NA	NA		4.4		5.2	3.9	3.9	10.4	4.2	
143	D	NA	NA	†	2.6	6.9	0.4	23.7	0.5	49.8	0.5	0.72

[a] α: α helix. *β*: *β* sheet. [b] Numbers: exposed area (Å^2). NA: no data available. [c] Not hydrogen bonded in the crystal structure. [d] Numbers are the average NOE contributions (s^{-1}) ± standard errors over three different pH values. No standard errors are given when values are from only one of the pH values due to overlap at other pHs. Dagger indicates that α protons are ±0.2 ppm from water frequency. [e] Observed rate constants in s^{-1} after correction for NOE contribution. Standard errors are within 10% except for residues with * (10−20%) and ** (20−30%). Blank: slower than the detection limit (<1.0 s^{-1}); NA: no data available. F: measurement is inaccurate due to too rapid exchange. [f] Protection factors (theoretical rate/measured rate). Values of 10^3 and higher were obtained from Loh et al.[22] [g] The ratio of exchange rate between pH 6.03 and 7.03 divided by $10^{\Delta pH}$ (=10).

observed in the so-called EX_1 limit,[32−34] where pH-insensitive breakage of hydrogen bonds is the rate limiting step. Because most amide protons observed in this study are non-hydrogen bonded, it is not clear whether this argument is applicable. One of the most intriguing findings is the complete lack of pH dependence of ^{77}Asn, which does not have any intramolecular hydroxyl group within 6 Å and no nearby titratable groups. This amide proton is facing inside of the protein, where the water molecule HOH 200[24] is located at the end of a deep cavity in the X-ray structure. It is therefore possible that the observed exchange rate is actually an intermolecular NOE or exchange contribution from the water molecule bound to the protein with a long lifetime.[35]

(2) Comparison of Measured Exchange Rates with Crystal Structural Properties. Hydrogen bondings and solvent-exposed areas of residues 9−141 deduced from X-ray crystallographic data[24] are shown in Table 1. Exposed areas are calculated from the contact of a probe (1.4 Å) with the van der Waals surface of hydrogen atoms. Hydrogen atoms are stereospecifically allocated from the crystal structure by X-PLOR.[36] Predicted exchange rates[2] for the random coil protein at pH 6.03 and the protection factors (=predicted value/measured value) for all pH values are also listed in Table 1. The predicted rates at pH 6.69 and 7.03 can be calculated simply by multiplying the values at pH 6.03 (sixth column) by 4.6 and 10, respectively. It is well-known that the exchange rates of backbone amide protons depend heavily on the amino acid side chain type. The method of Bai et al.[2] estimates the side chain effect and makes it possible to calculate the intrinsic exchange rate of each amide proton in random coil context. By using the protection factor, side chain effects are minimized and effects related to structure can be more directly appreciated.

The relationships between the X-ray structural data and the exchange rates and protection factors are summarized in Figure 4, parts A and B, respectively. To minimize the effect of intramolecular NOEs, especially from hydroxyl groups, results at high pH (7.03) are used in the following discussion. For residues exchanging too rapidly (^{116}Lys) or missing assignment (^{9}Lys) at pH 7.03, results at pH 6.03 are used. Several quick

(32) Hvidt, A.; Nielsen, S. O. *Adv. Protein Chem.* **1966**, *21*, 287−386.
(33) Roder, H.; Wagner, G.; Wüthrich, K. *Biochemistry* **1985**, *24*, 7396−7407.
(34) Pedersen, T. G.; Thomsen, N. K.; Andersen, K. V.; Madsen, J. C.; Poulsen, F. M. *J. Mol. Biol.* **1993**, *1993*, 651−660.
(35) Otting, G.; Wüthrich, K. *J. Am. Chem. Soc.* **1989**, *111*, 1871−1875.
(36) Brünger, A. T. *X-PLOR, Version 3.1: A System for crystallography and NMR*; Yale University Press: New Haven, 1992.

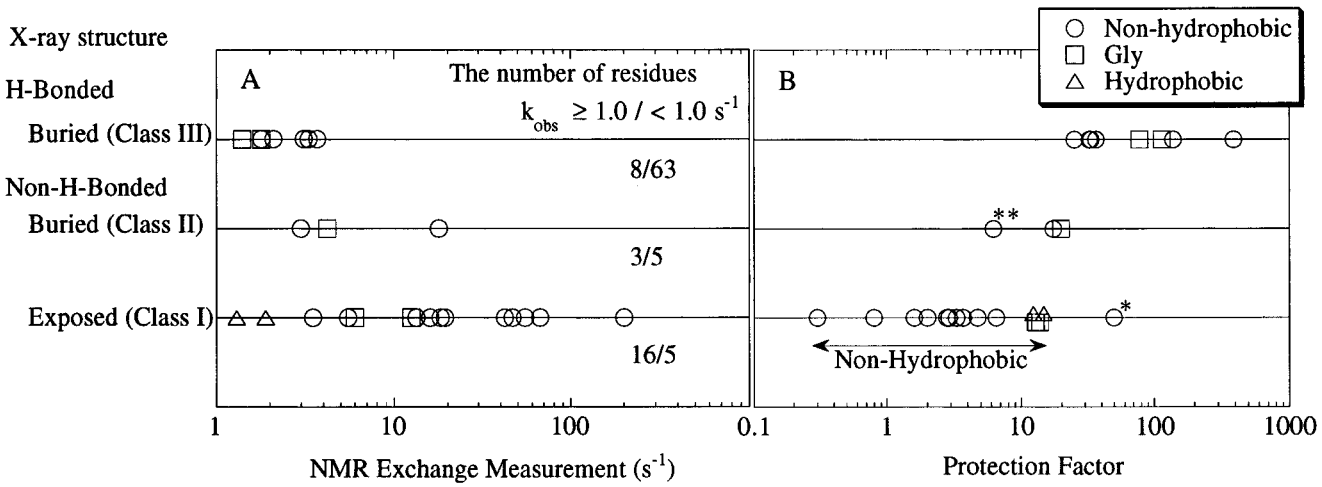

Figure 4. Correlation of X-ray structure and exchange rates (A) or protection factors (B) determined from NMR exchange measurements at pH 7.03. For those protons not assigned at pH 7.03, exchange rates are extrapolated from pH 6.03. Residues with asterisks (*: ^{82}Thr; **: ^{80}Gln) show marked discrepancies between structural information based on hydrogen exchange studies in solution and the crystal structure.

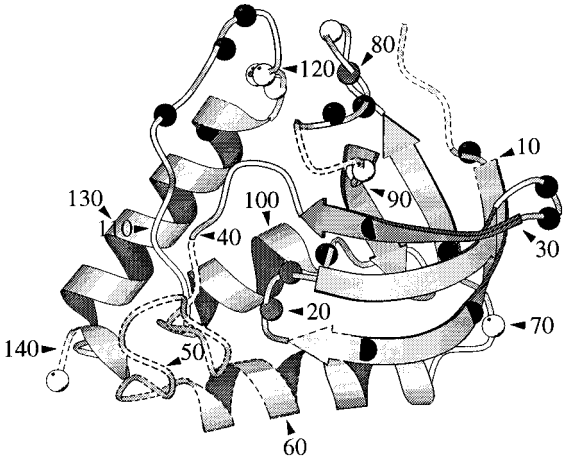

Figure 5. Ribbon diagram of SN showing positions of rapidly exchanging protons. Closed, gray, and open circles denote class I, class II, and class III protons, respectively. Unassigned residues are shown by dotted lines. The MOLSCRIPT program[40] was used for the diagram.

conclusions can be drawn from a brief inspection of Table 1 and Figure 4. First, most solvent-exposed and non-hydrogen-bonded amide protons in the crystal structure exchange fast enough to be detected. Second, some protons which are supposed to be buried and/or hydrogen bonded also show detectable exchange. Amide protons in the former type have significantly lower protection factors than the latter type. In the following discussion, amide protons are classified into non-hydrogen-bonded and exposed protons (denoted by class I), non-hydrogen-bonded and buried protons (class II), and hydrogen-bonded protons (class III) as shown in Figure 4.

Class I: Non-Hydrogen-Bonded and Exposed Protons. Most of the class I amide protons in the crystal exchange faster than the lower detection limit of 1.0 s^{-1} in solution at physiological pH (Figure 4A: 16 protons out of 21 in this category). These residues are located in N- and C-termini, loops, and turns, at the N-termini of α helices, or at the outer edges of β sheets (Figure 5: indicated by solid circles). The amide protons of residues 142 and 143 are also exchanging fast, indicating dynamic structure in this region. It is likely that most of the unassigned residues in the N- (1−8) and C-termini (144−149) and residues 41−61 are also in this category. It can be seen that the exchange rates of class I protons cover a much larger range than those of class III. This trend can be more clearly seen in Figure 4B, where side chain effects are minimized through the use of protection factors. Namely, all class I protons have protection factors below 15, which agrees well with findings by Orban et al.,[15] whereas those in class III have values greater than 25. A more detailed inspection of class I protons reveals that most of the protection factors are smaller than 10 except for Gly (^{29}Gly and ^{96}Gly) and the hydrophobic residues (^{14}Leu and ^{72}Ile). Three other hydrophobic residues (^{114}Val, ^{38}Leu, and ^{76}Phe) in class I have exchange rates below 1.0 s^{-1}. ^{114}Val showed finite exchange (0.5−1.0 s^{-1}) at pH 7.03, so that the protection factor is likely to be 15−30. ^{38}Leu and ^{76}Phe did not show detectable exchange, and the protection factors should be higher than 11 and 28 (=predicted exchange rates at pH 7.03/detection limit), respectively. In this regard, it is very intriguing to point out that our study on denatured SN[37] shows relatively high protection factors for Gly residues (1.6 ± 0.6) but not for hydrophobic residues (1.0 ± 0.2). This may suggest that there is an inherent difficulty in predicting the exchange rates of amide protons of Gly, probably due to its unique response to experimental conditions, which may lead to overestimation of the calculated exchange rates in the process of extrapolation from the experimental conditions used in the model system[2] to ours. On the other hand, consistently high protection factors of hydrophobic residues are likely to be induced by secondary or tertiary structure, such as packing of a remote hydrophobic side chain in the folded protein.

There are several exceptions in the behavior of class I protons. For example, ^{77}Asn has a protection factor that is too high to be classified as class I (25.9 at pH 7.03). The possible reason for the abnormal behavior was already discussed in the previous section. The residue ^{138}Asn also does not show detectable exchange (protection factor > 130), and should be classified to class II or III. Because ^{138}Asn is very close to the end of the sequence that could be observed by X-ray (up to ^{141}Ser), it is possible that the proton is buried or hydrogen bonded to a residue in 142−149. The non-hydrophobic residue ^{82}Thr, indicated by an asterisk in Figure 4B, has an abnormally high protection factor of 49.5. Since this proton has a small exposed area (0.7 Å), it may be buried or have very limited solvent exposure in solution, and should thus be classified as a class II proton. Discrepancies between structural information based on hydrogen exchange studies in solution and the crystal structure are commonly observed for protons at the surface of pro-

(37) Mori, S.; van Zijl, P. C. M.; Shortle, D. *Proteins; Struct., Funct., Genet.* In press.

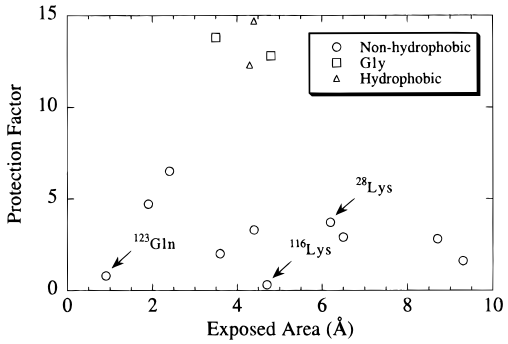

Figure 6. Correlation between exposed areas and protection factors at pH 7.03 for class I protons. For those protons not assigned at pH 7.03, protection factors at pH 6.03 are used.

teins[3,12,38,39] and, therefore, exchange studies are a useful additional tool for probing surface conformation of proteins in solution.[3]

Figure 4 clearly shows the influence of solvent exposure on proton exchange, which has been confirmed in many previous protein systems.[3,12,34,38,39] In agreement with earlier work,[14,15] we also found that many of the protection factors of exposed protons (class I) have a clear tendency of being higher than unity, indicating a possible variation in the degree of exposure. To test this, protection factors are compared to the exposed areas deduced from the X-ray structure in Figure 6. It can be seen that the correlation is poor ($r = 0.185$), partly because of the high protection factors of Gly and hydrophobic residues. However, the correlation among other residues is still poor ($r = 0.205$), and the existence of additional factors is clear. For example, ^{28}Lys and ^{116}Lys happen to have the same neighboring residue (Tyr) and predicted exchange rate (68 s^{-1}), and the exposed areas are comparable (6.2 and 4.7 Å^2, respectively). However, ^{116}Lys has a protection factor of 0.3 whereas ^{28}Lys has a factor of 3.7, and no correlation with exposed area is found. Another example is ^{123}Gln, which has a low protection factor (0.8), but a very limited exposed area. This poor correlation may result from the significant difference in exposed area between crystal and solution structure, or from dynamic factors, not immediately evident from the static structure. The effect of local electrostatic potentials may also contribute significantly.[4−6,15]

Class II: Non-Hydrogen-Bonded and Buried Protons. There are only eight residues in this class, ^{20}Gly, ^{21}Asp, ^{39}Val, ^{69}Ala, ^{80}Gln, ^{100}Asn, ^{101}Glu, and ^{109}Ala, of which three (^{20}Gly, ^{21}Asp, and ^{80}Gln: gray circles in Figure 5) show detectable exchange rates, and the protection factors are 6.2−19.8 (Figure 4). On the other hand, the deuterium−proton substitution studies[27] have found the protection factors for ^{39}Val, ^{100}Asn, ^{101}Glu, and ^{109}Ala to be more than 10^3 (see Table 1). Therefore, the range of protection factors in this class can vary significantly, and the variation may reflect the extent of exposure of each proton. For example, ^{80}Gln, indicated by two asterisks in Figure 4, has a protection factor of 6.2. Considering the fact that most atoms of ^{80}Gln, including the nitrogen of the amide group, are exposed, it is highly likely that the amide proton of ^{80}Gln is not only non-hydrogen bonded but also solvent exposed. On the other hand, ^{20}Gly and ^{21}Asp are almost entirely buried, but still show rapid exchange with the expected pH dependence. This indicates that they experience significant exposure to solvent hydroxyl ions due to structural fluctuations, which is in agreement with previously reported structural flexibility in solution in a large loop−turn region in residue 40−53, behind which the amide protons of ^{20}Gly and ^{21}Asp are located in the X-ray structure (Figure 5).[25,26]

Class III: Buried and Hydrogen-Bonded Protons in the Crystal Structure. Some protons which are buried and hydrogen bonded show detectable exchange rates, but have significantly higher protection factors. Among these are ^{70}Lys, ^{79}Gly, ^{86}Gly, ^{87}Arg, ^{118}Asn, ^{119}Asn, ^{120}Thr, and ^{141}Ser, and the protection factors are 25−390. These residues are located predominantly in loop or turn regions (open circles in Figure 5). Most notable are the loop−turn regions in residues 79−87 and 113−123. Knowing that these two regions are facing each other at the surface of the protein and forming main chain to side chain hydrogen bonds (79 N → 118 O, 118 N → 80 O, 120 N → 77 O), it can be deduced that this region of the protein is not stable in solution at physiological pH. On the other hand, it can be seen in Table 1 that there are many protons which have protection factors more than 10^3, probably due to more stable hydrogen bonds and/or a high degree of solvent inaccessibility. These protons are mainly located in α helices and β sheets. All hydrogen-bonded hydrophobic residues in class III exchange below the detection limit.

(3) Comparison with Other Solution NMR Dynamics Studies. Data from a deuterium−proton substitution study on ligand-free SN[27] are included in Table 1. The behavior for liganded SN has also been studied,[25] and both studies indicate that all protons in class I and II exchange more rapidly than the detection limit. On the other hand, the substitution study could measure the exchange rate of most protons in category III. Therefore these methods are complementary. In a relaxation study of ^{15}N in liganded SN,[26] extraordinary short T_2 values were observed for residues 22, 23, 52, and 53, which could be due to motional averaging. Although the presence of a ligand in this study precludes direct comparison with our measurements, postulated flexibility at the edge of the second β sheet (residues 22 and 23) agrees with rapid exchange of protons at residues 20 and 21, which are buried in the X-ray structure.

(4) Comparison with *B*-Factors. The crystallographic *B*-factor is a measure of the sharpness of localization of electron density for each atom, which, among other factors, includes contributions from structural dynamics. Although exchange measurements are not a direct indicator of this dynamic, it is likely that they reflect regional flexibility caused by the absence or breakage of hydrogen bonds. Therefore, it is interesting to compare these two parameters. In Figure 7, exchange rates at pH 7.03 are compared with *B*-factors obtained from the X-ray structure by Hynes et al.[24] It can be seen that amide protons in regions with larger *B*-factors (>20) such as the N- and C-termini, residues 29−31 and 114−117, tend to exchange rapidly. Rough categorization of *B*-factors reveals some extent of correlation between the two parameters as shown in Table 2. However, the large standard deviations indicate that their correlation is not simple. For example, most amide protons in the α-helices at residues 62−68 and 121−135 do not exchange rapidly because of their stable hydrogen bonds even though they have relatively high *B*-factors (∼15). This may imply that these α-helices experience structural fluctuation as a whole unit, leaving individual backbone hydrogen bonds unaffected. On the other hand, amide protons in residues 20 and 21 show detectable exchange in spite of their low *B*-values. As discussed in the previous section, their exchange may be caused by dynamic disorder of residues 40−52, which is probably more substantial in solution than in the crystal.

(38) Pedersen, T. G.; Sigurskjold, B. W.; Andersen, K. V.; Kjær, M.; Poulsen, F. M.; Dobson, C. M.; Redfield, C. *J. Mol. Biol.* **1991**, *218*, 413−426.

(39) Radford, S. E.; Buck, M.; Topping, K. D.; Dobson, C. M.; Evans, P. A. *Proteins; Struct., Funct., Genet.* **1992**, *14*, 237−248.

(40) Kraulis, P. *J. Appl. Crystallogr.* **1991**, *24*, 946−950.

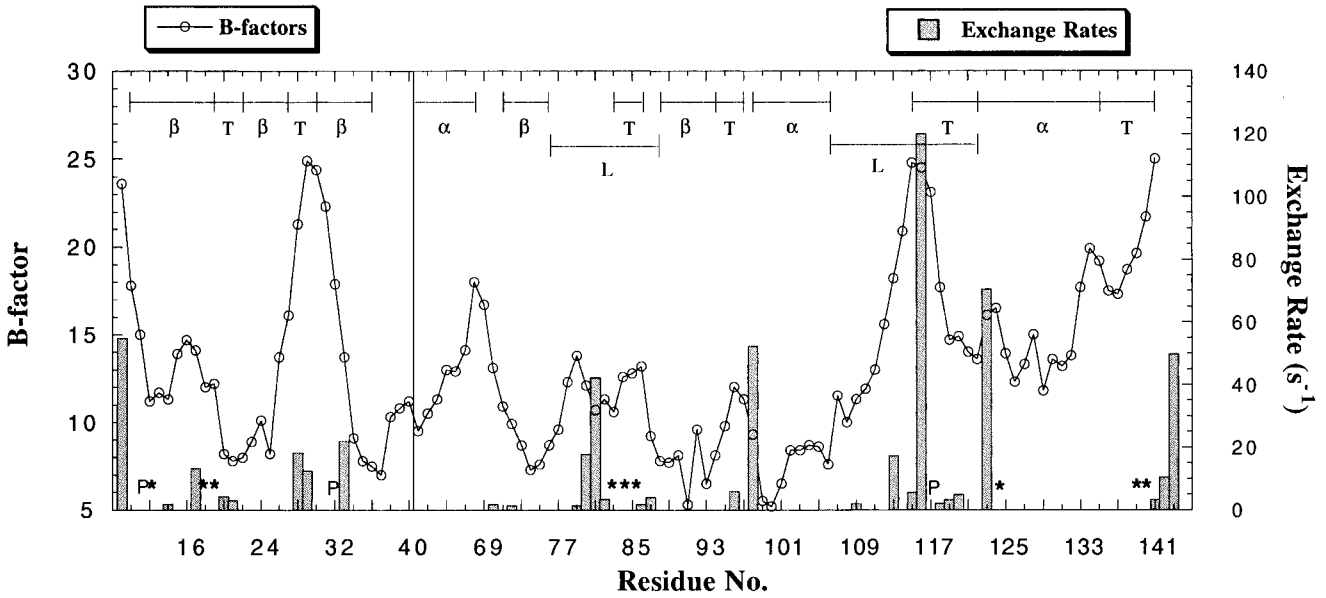

Figure 7. Comparison of *B*-factors and exchange rates. *B*-factors are obtained from the PDB file from Hynes et al.[24] Exchange rates are at pH 7.03. Exchange rates of residues 9 and 116 are calculated values from lower pH. No data are available for residues with an asterisk. P indicates proline.

Table 2. Correlation between *B*-Factor Ranges and Exchange Rates (s^{-1}) at pH 7.03

B-factor	rates
5−10	1.9 ± 9.0
10−15	3.3 ± 8.2
15−20	7.2 ± 19.6
20−25	30.5 ± 52.9

Conclusions

NOE-corrected proton exchange rates were measured for SN in solution near neutral pH and correlated with structural properties. From the results, several conclusions can be drawn: (1) Non-hydrogen-bonded and exposed residues (class I) have protection factors of 1−15 for non-hydrophobic residues and 10 or higher for hydrophobic residues. Among non-hydrophobic residues, Gly residues tend to have higher protection factors (10−15), whereas other residues are below 10. (2) Protection factors for buried and non-hydrogen-bonded protons (class II) vary over a wide range (12 to 10^4). Low protection factors (<25) may indicate significant fluctuations in structure and substantial solvent exposure. (3) Some hydrogen-bonded protons (class III) show rapid exchange, and the protection factors are 25−390. This indicates labile hydrogen bonds and solvent exposure by structural fluctuation. On the other hand, many class III protons are observed in α helices and β sheets[27] or hydrophobic residues and have protection factors $>10^3$. Although a good correlation between NMR exchange measurements at neutral pH and X-ray structural properties is observed, discrepancies are also found for several residues such as residue ^{80}Gln (class II in X-ray; class I in NMR) and ^{82}Thr and ^{138}Asn (class I in X-ray; class II or higher in NMR). The pH-dependence studies also revealed unusual behavior of ^{77}Asn, possibly due to interaction with a tightly bound water molecule.

The data on SN presented here only provide a first indication of classification, and it is of great interest to see whether these trends are also found in other proteins. In this respect, it is noteworthy that Orban et al.[15] found protection factors of less than 15 for most class I protons in the B1 and B2 domains of protein G. However, it should be pointed out that existence of hydrogen bonds may not necessarily be monitored by discrete protection factors due to structural dynamics. As Gryk et al.[17] and Finucane and Jardetzky[13] demonstrated in *trp* Repressor, a region of protein may undergo conformational fluctuation with unstable hydrogen bonds. When this is the case, our analysis will yield average exchange rates for the contributing conformations, which may lead to a wide range of protection factors between unity to more than 25, depending on the population of the hydrogen bonded and non-hydrogen bonded species. Furthermore, protection factors may have uncertainties due to extrapolation from experimental conditions used in the original work[2] (5 °C, mostly pH <5.0) to the conditions used for magnetization transfer study (39.4 °C, pH 6.03−7.03 in our study).[39] Therefore, the range of protection factors observed in our study may not be completely reproduced in other systems, especially at the boundaries between classes.

Nevertheless, the data indicate that classification with use of protection factors should be a useful tool for interpreting exchange measurements and deducing surface conformation at neutral pH. For example, a proton with a protection factor of less than 10 (except for Gly and hydrophobic residues) strongly indicates the absence of stable hydrogen bonding. A protection factor well above 25 implies the existence of hydrogen bonds and the proton is classified as class III. Many applications should follow with use of these criteria. For example, if a NMR structural study did not yield enough constraints in some region, this classification could be used to judge whether the region really lacks stable hydrogen bonds. Stable residual structures in partially unfolded proteins are also expected to be detected and classified in class III. The impact of various environmental conditions on structural dynamics such as pH, temperature, and salt conditions can also be assessed. Another topic of interest is the study of protein−ligand interactions.

Acknowledgment. This study was supported by the National Institutes of Health Grant RR11115 (NCRR) and the Lucille P. Markey Charitable Trust. We thank Dr. David Shortle for the sample preparation and the critical reading of the manuscript. We are grateful to Dr. S. W. Englander (University of Pennsylvania) for kindly providing the spreadsheets used for calculating the random-coil exchange rates.

JA963351F